Influence of Textural Properties of Divinylbenzene Copolymers on the Immobilization of Lipase B from *Candida antarctica*

Tatiane S. Ribeiro[1], Ezaine C. C. Torquato[1], Eliane P. Cipolatti[2,3], Martina C. C. Pinto[4,5], Evelin A. Manoel[3,4],

Mônica R. C. Marques[6], Denise M. G. Freire[4], José Carlos Pinto[5], Luciana C. Costa[1]*

[1]Centro Universitário Estadual da Zona Oeste (UEZO), Programa de Pós-graduação em Ciência e Tecnologia Ambiental (PPGCTA), Rio de Janeiro, RJ, Brasil.
[2]Universidade Federal Rural do Rio de Janeiro, Instituto de Tecnologia, Departamento de Engenharia Química, CEP 23890-000, Seropédica, RJ, Brasil.
[3]Universidade Federal do Rio de Janeiro, Faculdade de Farmácia, Departamento de Biotecnologia Farmacêutica, Rio de Janeiro, RJ, Brasil.
[4]Universidade Federal do Rio de Janeiro, Departamento de Bioquímica, Instituto de Química, Rio de Janeiro, RJ, Brasil.
[5]Universidade Federal do Rio de Janeiro, Programa de Engenharia Química / COPPE, Rio de Janeiro, RJ, Brasil.
[6]Universidade do Estado do Rio de Janeiro, Programa de Pós-graduação em Química, Rio de Janeiro, RJ, Brasil.

Previous studies have investigated the preparation of heterogeneous biocatalysts based on the immobilization of lipases on distinct types of supports. However, few works have investigated the influence of the textural properties of these supports on the immobilization parameters. Thus, the present article reports the preparation of copolymers based on divinylbenzene by aqueous suspension polymerizations, using different amounts of porogenic agents to prepare particles with distinct textural properties. The particles were used for immobilization of lipase from *Candida antarctica* fraction B and the performance of the biocatalysts was evaluated in hydrolysis reactions, using *p*-nitrophenyl laurate as substrate. The use of Sty/DVB particles resulted in higher immobilization yields (89.5% and 99.2%) and higher hydrolytic activities, when compared to the Sty/VBC/DVB particles. Particularly, the increase of the pore diameters of the particles resulted in higher immobilization yields. Also, the hydrolytic activities depended simultaneously on the average pore diameter, porosity, and specific area (the most influential variable) of the supports. Thus, it was observed that the distinct morphological features of the polymer support can exert significant and conflicting effects on the final biocatalyst performance, since the specific surface area is normally expected to decrease with the increase of the average pore size.

Keywords: *Styrene-divinylbenzene copolymers, porous polymers, heterogeneous biocatalysts, CALB, enzyme immobilization*

1. Introduction

Lipases (triacylglycerol acyl hydrolases EC 3.1.1.3) have been widely used in many areas for the manufacture of pharmaceuticals, foods and chemicals. These enzymes are robust and highly active. Besides this, the widespread use of these enzymes in industrial processes is also due to the availability of commercial preparations, the broad spectrum of substrates that can be transformed into commercial products, the possible application in several reactions, and the easy immobilization on solid supports[1-5].

Nevertheless, the use of free enzymes in solutions can be very disadvantageous in actual commercial environments, due to enzymatic stability problems and difficult separation of the enzyme from the final product, which can lead to high operating costs[6]. On the other hand, the immobilization of enzymes on solid supports can enhance the enzymatic stability under different operational conditions and allow the recovery and reuse of the biocatalysts, leading to lower operating costs[7]. Additionally, the immobilized biocatalysts can be used in continuous processes, reducing the need for additional product purification steps. For these reasons, several industrial sectors already employ immobilized enzymes to manufacture pharmaceuticals, chemicals and foods[8].

Although the immobilization of enzymes on solid supports can be achieved through various strategies (such as occlusion, crosslinking, trapping, and covalent bonding), physical adsorption certainly is the commonest immobilization procedure[9]. Consequently, many studies have investigated the adsorption of lipases on various hydrophobic surfaces at

*e-mail: luciana.cunha.costa@gmail.com

low ionic strength, through some sort of interfacial activation mechanism. This strategy allows the immobilization of the enzymes in their open and active forms and the sequential immobilization, purification, stabilization and hyperactivation of the enzymes in the same reactor[2,8,9].

Styrene/divinylbenzene copolymer particles with porous structures obtained by aqueous suspension polymerization can be good candidates to support enzymes. The interest in such polymers can be explained by the simplicity of the polymerization technique, the low cost of the monomers, the possibility of preparing particles with different properties (size distribution, surface area, pore volume, pore diameter), and ease of modifying these structures, through functionalization reactions using different functional groups[10]. For these reasons, many works have already described the preparation of heterogeneous biocatalysts based on styrene/divinylbenzene copolymer particles and have studied the relationship between the immobilization parameters and activity of the produced biocatalysts[11-20]. The kinetic behavior of reactions catalyzed by heterogeneous biocatalysts can be affected by many process parameters, including conformational and environmental conditions, related to the enzyme immobilization process. Parameters such as temperature, pH and ionic strength can cause modifications of the geometric and electronic features of enzyme molecules, changing their spatial configuration and activity[21]. Environmental effects, related to diffusion and mass transfer limitations of substrates and products, can also significantly affect the performance of biocatalysts. In particular, mass transfer constraints can be related to liquid-liquid diffusion and surface diffusion (or external diffusional restriction, EDR) limitations and intraparticle diffusion (or internal diffusional restriction, IDR), when the enzyme immobilization is carried out on gels and porous particles[22]. These mass transfer constraints are often related to morphological characteristics of the supports, such as the specific surface area, pore volume, average pore size and pore size distribution, along with other factors related to the swelling properties of the support in the reaction medium and polydispersity of the particles[23-26]. For these reasons, the performance of heterogeneous biocatalysts depends on the properties of the enzymes, characteristics of the reaction medium, reaction conditions, and physical-chemical characteristics of the supports. Thus, all these factors can simultaneously affect the enzyme immobilization yields, the observed biocatalyst activities, and the short and long-term stabilities of the prepared biocatalyst[1].

The manufacture of heterogeneous biocatalysts based on immobilized supports has attracted strong interest in both the academic and industrial communities. Many studies have explored the correlations between the textural properties of the analyzed supports and the immobilization parameters, using the important commercial lipase B from *Candida antarctica*, CALB[4,22-26].

Li et al.[26] prepared biocatalysts based on the immobilization of lipases on polystyrene beads with distinct average pore sizes (gigaporous, macroporous or mesoporous particles). They observed that the enzyme molecules could access the pores of giga and macroporous polymer particles after having been immobilized on the external and internal surfaces of these particles, resulting in highly active and stable biocatalysts (in terms of thermal stability, storage stability, and reusability).

Pinto et al.[4,23,24] and Cunha et al.[25] conducted several studies involving the immobilization of lipases on core-shell polymer microparticles with distinct morphological characteristics, while Pinto et al.[24] studied the immobilization of lipases on nanoparticles produced through emulsion polymerization. Specifically, these works showed the strong relationship between the immobilization parameters and the specific surface areas of the supports, but also revealed the relatively small effect of the average pore size on the final performance of the biocatalysts.

More recently, Torquato et al.[27] investigated the use of porogenic agents to produce porous Sty/DVB copolymer microparticles with different morphological features through aqueous suspension polymerization, but did not use these particles as supports for enzyme immobilization. Indeed, previous studies have not evaluated the use of porous particles produced through aqueous suspension polymerization in the presence of porogenic agents as supports for enzyme immobilization and production of biocatalysts[11-20]. For this reason, the correlation between the textural properties of the obtained polymer beads and the immobilization parameters for these materials is not yet known. Considering the effects that the polymerization parameters can exert on the support morphology and pore structures, this investigation can be of significant importance for biocatalyst manufacturing technology.

Based on the previous remarks, the present work evaluated the influence of the textural properties of styrene/divinylbenzene (Sty/DVB) and styrene/vinylbenzyl chloride/divinylbenzene (Sty/VBC/DVB) copolymer supports, obtained through aqueous suspension polymerization in the presence of two different porogenic agents, on the immobilization of lipase B from *Candida antarctica* (CALB) and on the final performance of the biocatalysts. The results indicate that the increase of the pore diameters can lead to higher immobilization yields, although the final hydrolytic activities can depend simultaneously on the average pore diameter, porosity, and specific area (the most influential variable) of the analyzed supports.

2. Experimental

2.1. Chemicals

Styrene and divinylbenzene monomers were kindly donated by Nitriflex Industria Comércio SA® (Rio de Janeiro, Brazil) and used after washing with a 5% w/v aqueous NaOH solution. 4-vinylbenzyl chloride (VBC) (90%) was supplied by Sigma-Aldrich (Missouri, USA) and used as received. 2,2 azobisisobutyronitrile (AIBN) was purchased from MigQuimica® (São Paulo, Brazil) and used after recrystallization in methanol. Heptane (PA grade), toluene (PA grade), and acetonitrile (99.9%) were supplied by Sigma-Aldrich (Missouri, USA). Dimethyl sulfoxide (99.9%) was purchased from Tedia (Ohio, USA). Ethanol (95%) and oleic acid (PA) were purchased from Synth (São Paulo, Brazil). Poly(vinyl alcohol) (PVA) (88% hydrolysis degree) and sodium chloride were supplied by Vetec Química Fina Ltda. (Rio de Janeiro, Brazil). *p*-Nitrophenyl laurate

Influence of Textural Properties of Divinylbenzene Copolymers on the Immobilization of Lipase B from
Candida antarctica

3

(98.0%) (*p*-NPL) was supplied by Sigma-Aldrich (Missouri, USA). Lipase from *Candida antarctica* fraction B (CALB) was purchased from Novozymes (Bagsværd, Denmark). These reagents were used as received.

2.2. Synthesis of crosslinked copolymer particles

Styrene/divinylbenzene (Sty-DVB) and styrene/vinylbenzyl chloride/divinylbenzene (Sty/VBC/DVB) copolymers were produced through aqueous suspension polymerization in a 1000 mL three-necked round bottom reactor, equipped with a reflux condenser and digital mechanical stirrer. The aqueous phase was prepared by dissolving PVA (0.5% w/v) and NaCl (0.5% or 1% w/v) in distilled water. The volumetric ratio between the aqueous and organic phases was always equal to 4:1 (v/v). Sty/DVB copolymers were prepared with 0.12 mol of Sty and 0.18 mol of DVB. Sty/VBC/DVB copolymers were synthesized with 0.06 mol of Sty, 0.06 mol of VBC, and 0.18 mol of DVB.

The organic phase was prepared by dissolving AIBN (1% mol/mol related to monomers) in a solution containing the monomers and a mixture of toluene and heptane (20/80 or 80/20% v/v) as porogenic agent. The volume ratio between the monomer and porogenic agent mixtures was equal to 1:1.5 v/v. The organic phase was dispersed in the aqueous phase and the polymerization reaction was performed under continuous stirring of 230 rpm at 80 °C for 24 h. The produced beads were then filtrated and washed with distilled water, ethanol and acetone to eliminate residual monomers and diluents. Finally, the microspheres were dried at 60 °C for 24 hours.

2.3. Characterization of crosslinked copolymer particles

The copolymer beads were characterized through the determination of specific surface area, pore volume, and average pore diameter (BET analyzer, Micromeritics model ASAP 2020). The isotherms were plotted by correlating the amount of adsorbed gas on the copolymer particles (cm^3/g^{-1}) as a function of the relative pressure (P/P$_0$), employing the BET equation and the BJH method[28,29]. Apparent density of the particles was determined by the graduated cylinder method according to ASTM D1895[30].

The particle size distribution was characterized by employing a Malvern Hydro 2000S Mastersizer.

The morphology of the particles was analyzed through optical and scanning electron microscopies. Optical microscopy was performed with an Axiovert 40 MAT microscope (Carl Zeiss) equipped with a digital camera (AxioCamMRc 5). Scanning electron microscopy (SEM) was performed with a JEOL-JSM 6460 LV system operating at 20 keV, with magnification of 10 000 x. For SEM, the samples were spread on a conductive tape and sputtered with gold.

2.4. Immobilization of CALB on crosslinked copolymer particles

The enzyme immobilization procedure was based on the physical adsorption of lipase on the surface of the supports, as described in several studies[4,22-24,31,32]. The first step of the immobilization process was the pretreatment of the copolymers with ethanol (95%) (30 mL), distilled water (30 mL), and sodium phosphate buffer solution (5 mM and pH 7). Following Cunha et al.[25], this procedure was carried out to eliminate residual monomers and facilitate the penetration of the enzyme solution into the support structure. Enzyme solutions were prepared by diluting the commercial suspension of lipase *Candida antarctica* fraction B (CALB) (0.5 mL) in sodium phosphate buffer (5 mM, pH = 7.0) (9.5 mL). The enzyme immobilization procedure was performed through the addition of the enzyme solution (10 mL) to the pretreated support (1 g) (initial enzymatic activity of 180 U g$_{support}^{-1}$). Immobilization was carried out at 30 °C under stirring of 40 rpm for a total time of 5 hours.

2.5. Monitoring the immobilization procedure

The immobilization procedure was monitored by determining the reduction of the hydrolytic activity of the free enzymes still present in the supernatant, using *p*-nitrophenyl laurate (*p*-NPL) as substrate. The formation of the chromophore *p*-nitrophenol was accompanied by monitoring the absorbances at 412 nm (Shimadzu UV-1800 spectrophotometer). Aliquots of the enzyme solution (50 µL) were collected from the supernatant during the immobilization procedure (0, 0.5, 1, 2, 3, 4, and 5 h). These solutions were added to a substrate solution containing *p*-NPL in acetonitrile/dimethyl sulfoxide solution (1:1 v/v) and sodium phosphate buffer (25 mM, pH = 7.0). Analyses were performed at 30 °C, under mild agitation, in triplicate[4,22-24,31,32].

An enzyme unit (1 IU) is defined as the amount of enzyme required to produce 1 µmol of *p*-NP per minute[4]. The hydrolysis activity and immobilization yield were calculated by using the equations described in Table 1.

2.6. Determination of the hydrolytic activity of the biocatalyst

The hydrolytic activity of the biocatalysts was determined using *p*-nitrophenyl laurate (*p*-NPL) as a substrate. The hydrolysis reaction was carried out at 30 °C, under mild agitation, and *p*-NPL (250 µL) and sodium phosphate buffer (25 mM, pH 7.0) were added to the cuvette. The reaction was started by adding 10 mg of biocatalyst to the medium. The absorbances were determined (412 nm) for 3 minutes. The equations in Table 1 were employed to determine the hydrolytic activity and retention of enzyme activity of the biocatalysts, respectively[4,22-25,31,32].

3. Results and Discussion

The success of the immobilization process depends on the catalytic properties of the enzymes and the physicochemical properties of the supports. Thus, the performance of the prepared heterogeneous biocatalysts depends on the characteristics of these two components and the immobilization conditions, which affect the spatial configuration of the immobilized enzyme molecules, immobilization yields, mass transfer effects, and operational stability of the final biocatalysts[1,22-25]. The physical-chemical properties of the polymeric supports are determined essentially by the experimental conditions employed in the polymerization reactions, related to the monomer compositions, polymerization strategy, and reaction parameters (such as temperature and stirring speed).

Table 1. Equations used for characterization of immobilized enzymes properties[4, 22-24,31,32]

Equation Title	Equation
Hydrolytic activity of the soluble enzyme	$$A_H{}^{a)} = \frac{\left(\frac{Abs}{min}\right)^{b)} * V_f{}^{c)} * f^{d)}}{V_e{}^{e)}}$$
Immobilization yield (IR)	$$IY^{f)}(\%) = \frac{U_{theo} * 100}{U_e} \quad U_{theo}{}^{g)} = U_e{}^{h)} - U_s{}^{i)}$$
Hydrolytic activity of the biocatalyst	$$A_{imohyd}{}^{j)} = \frac{\left(\frac{Abs}{min}\right) * V_f * f}{m_e{}^{k)}}$$
Recovered activity	$$R_a{}^{l)} = \frac{A_{imohyd} * 100}{U_{theo}}; U_{theo} = U_e - U_s$$

[a)] Hydrolytic activity (UI mL^{-1}); [b)] angular coefficient of the straight line obtained with the advance of the hydrolysis reaction; [c)] final volume of the reaction medium (mL); [d)] factor obtained from the *p*- nitrophenol calibration curve; [e)] enzyme volume (mL); [f)] immobilization yield (%); [g)] activity of the enzyme theoretically immobilized on support (U g$_{support}$$^{-1}$); [h)] enzymatic activity of the solution at the start of immobilization (U g$_{support}$$^{-1}$); [i)] enzymatic activity of the solution at the end of immobilization (U g$_{support}$$^{-1}$); [j)] hydrolytic activity of the biocatalyst (UI g$_{bio}$$^{-1}$); [k)] mass of biocatalyst (g); [l)] recovered activity (%) obtained through correlation between hydrolytic activity of the biocatalyst and activity of the enzyme theoretically immobilized on support.
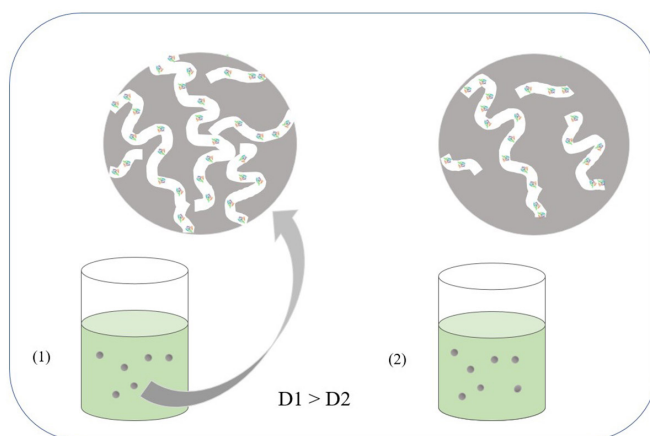
Figure 1. Schematic representation of the effect of the pore diameter about access of the enzymatic solution from the bulk of solution until the internal surface of the particles (a) particles with high pore diameter (D1) or (b) particles with low pore diameter (D2).

Two of the parameters that affect the morphological characteristics of the polymer microparticles prepared through aqueous suspension polymerization are the type and amount of porogenic agent added to the dispersed organic phase. It is possible to prepare supports with distinct pore diameter distributions by varying these variables[33].

The porosity degree of the polymer, particularly the pore diameters of the particles, influences the process of enzyme diffusion and consequently the extent of the reactions catalyzed by the immobilized enzymes. Thus, it is possible to suppose that the access of the enzymatic solution from the bulk of the solution to the internal surface of the particles was more favorable for copolymer 1 than copolymer 2, since copolymer 1, prepared by using high amount of a non-solvating solvent as porogenic agent, had higher pore diameters than copolymer 2 (D1>D2), (Figure 1).

## 3.1. Morphological characteristics of the copolymer microparticles

Batches of Sty/DVB (0.12:0.18 mol/mol) and Sty/VBC/DVB (0.06:0.06:0.18 mol/mol) copolymer microparticles were synthesized by varying the composition of the porogenic mixture, with toluene:heptane mixtures (80:20 and 20:80 v/v) as porogenic agents. Consequently, supports with different compositions and morphological features were produced, as shown in Table 2 and Figures 2, 3 and 4.

Aqueous suspension polymerization normally produces polymeric particles with broad size distribution. It is well known that the size of the particles and particle size distribution produced by aqueous suspension polymerization are related to parameters such as the type of initiator, temperature of the medium, stirring speed and amount of suspending agent[34]. However, it is necessary to evaluate if changes in

Influence of Textural Properties of Divinylbenzene Copolymers on the Immobilization of Lipase B from
Candida antarctica

5

Table 2. Bulk densities, specific surface areas, pore volumes and average pore diameters of copolymers

Supports	Tol:n-Hep[a)] [v/v]	d_{ap}[b)] [g cm^{-3}]	S[c)] [m^2 g^{-1}]	V_p[d)] [cm^3 g^{-1}]	D[e)] [Å]
Sty/DVB (1)	80:20	0.5	285	0.27	41
Sty/DVB (2)	20:80	0.5	319	1.06	187
Sty/VBC/DVB (3)	80:20	0.5	193	0.74	162
Sty/VBC/DVB (4)	20:80	0.4	49	0.24	180

[a)]Toluene:n-heptane composition; [b)]bulk density; [c)]specific surface area; [d)] pore volume; [e)]average pore diameter.
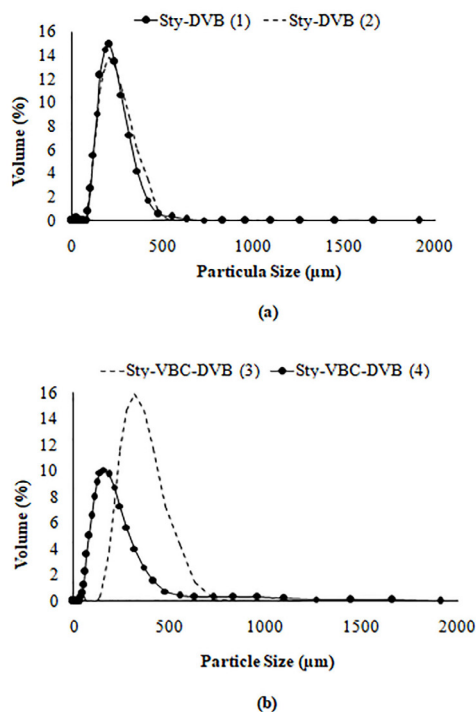
Figure 2. Particle size distribution of copolymers: (a) Sty/DVB (1) x Sty/DVB (2), (b) Sty/VBC/DVB (3) x Sty/VBC/DVB.

the composition of the porogenic mixture or monomeric mixture will cause significant changes in particle size and polydispersity. The data obtained here showed, as expected, the absence of significant variations in particle size or polydispersity related to modifications in diluent composition (Figure 2a) or monomeric composition (Figure 2b). Data of particle size distribution for Sty-DVB and Sty-VBC-DVB copolymers showed a higher proportion of the particles with sizes between 150 and 300 μm.

As described in the literature, the characteristic physisorption isotherms of solid particles can display different formats, which are classically grouped into six main types that can be associated with the porous structure of the analyzed particles[28,35-39]. In particular, the characteristic Type IV and V isotherms show hysteresis between the adsorption and desorption processes. However, Type V isotherms can generally be associated with porous materials that do not exhibit pronounced microporosity[38]. Thus, the occurrence of hysteresis between the observed

adsorption and desorption processes indicates that the copolymers manufactured in this work exhibited the characteristic Type IV isotherm adsorption profile, as observed in Figure 3. Many authors have reported that this type of isotherm is characteristic of materials that predominantly contain mesopores[28,35-39]. For instance, Zhang et al.[38] stated that this type of isotherm can indicate the existence of connections between pores of different sizes, in the micro and mesoporous domains.

It is also possible to observe in Figure 3a and 3b that the isotherm profile of Sty/DVB copolymers changed significantly when the diluent composition was altered. This clearly suggests that the use of diluent affected the porous structure of the particles. On the other hand, this was not observed with Sty/VBC/DVB copolymers (Figure 3c and Figure 3d), indicating that addition of the VBC comonomer did not significantly affect the thermodynamic interactions of the diluent with the reaction medium. For these materials, there was a small variation in the amount of N_2 adsorbed over a wide range of P/P_0. Hysteresis loops can exhibit a wide variety of shapes, typically grouped into four main types: H1, H2, H3 and H4. In general, the hysteresis indicated by the curves of the Sty/DVB (2) and Sty/VBC/DVB (3) and Sty/VBC/DVB (4) copolymers (Figure 3) had Type H3 isotherms. This type of hysteresis is related with structures containing aggregates of plate-like particles containing slit-shaped pores and also with structures containing a pore network with macropores that are not completely filled with condensate[35,37].

Table 2 shows that the increase of the heptane content of the porogenic agent led to an increase in specific surface area, pore volume and pore diameter of Sty/DVB microparticles. However, the increase of the pore volume (393%) was much larger than the increase of the specific surface area (12%), indicating increase of the average pore size, as also confirmed in Table 2 and the following equations:

$$S = N l \pi D \tag{1}$$

$$V_p = N l \pi \frac{D^2}{4} \tag{2}$$

where S is the surface area, N is the number of pores per mass of particles, l is the pore length, D is the pore diameter, and V_p is the pore volume. Equations 1 and 2 assume the cylindrical pore shape and the small contribution of the particle surface for characterization of S. Also,

$$\frac{V_{p1}}{V_{p2}} = \frac{S_1}{S_2} \frac{D_1}{D_2} \tag{3}$$
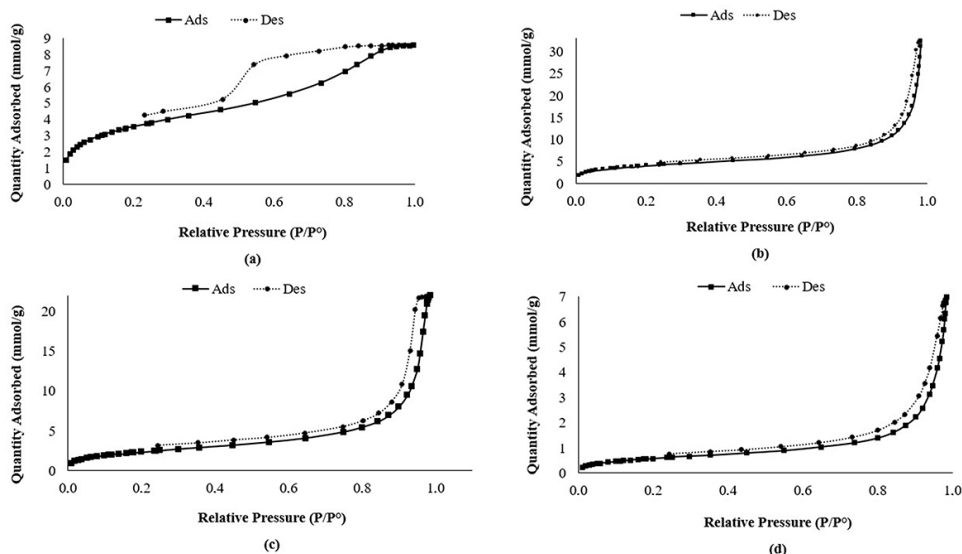
Figure 3. Adsorption and desorption isotherms of the polymer supports: (a) Sty/DVB (1), (b) Sty/DVB (2), (c) Sty/VBC/DVB (3) and (d) Sty/VBC/DVB (4).

so that two of the measured morphological parameters of two distinct particles (1 and 2) (pore diameters and surface area, for example) are sufficient to explain the observed variations of the other ones (pore volume for example).

Both Sty/DVB copolymers were characterized by similar bulk densities (Table 2), indicating that these densities were significantly affected by particle packing and particle size distribution (otherwise, sample Sty/DVB (2) should present lower bulk density, given its much larger pore volume).

Figure 4 depicts optical and SEM micrographs of these two copolymer samples. Sty/DVB (1) presented a translucent aspect, whereas Sty/DVB (2) had an opaque appearance. SEM microscopies shows that Sty/DVB (2) contained a more porous structure than Sty/DVB (1) copolymer, confirming the data on specific surface area and pore volume of these two samples.

As described previously, N_2 adsorption experiments conducted with Sty/DVB copolymer samples (Figure 3) showed that the hysteresis behavior was more pronounced for Sty/DVB (1) (prepared with diluent composition of 80:20 toluene:n-heptane v/v) than for Sty-DVB (2) sample (prepared with diluent composition of 20:80 toluene:n-heptane v/v), indicating significantly different condensation and evaporation processes in these two cases. In particular, the presence of narrow pores in the first sample can induce the development of the well-known tensile strength effect (TSE), which occurs when larger pores are blocked and nitrogen must evaporate through very smaller pores, at pressures below P/P_0 0.5[36,38]. This can explain the sharp peaks of the pore size distributions of Figure 5.

The pore size distributions for these two copolymers (Figure 5) showed that Sty/DVB (1) copolymer had a narrow pore distribution whereas Sty/DVB (2) copolymer presented larger pores, indicating that the increase of the heptane content of the porogenic agent also led to a significant increase of the polydispersity of the pore size distribution The data on

pore diameter of these two materials (Table 2) corroborate these results. Sty/DVB (1) had average pore diameter of 41 Å while Sty/DVB (2) presented average pore diameter of 187 Å.

The increase of the heptane content of the porogenic agent in samples Sty/VBC/DVB (3) and Sty/VBC/DVB (4) resulted in the reduction of the specific surface area (75%) and of the pore volume (68%) (Table 2), accompanied by the larger dispersity of the pore size distribution (Figure 5). The adsorption isotherms obtained for these two materials revealed similar profiles (Figure 3), and the less pronounced hysteresis behavior in these two cases, indicating the presence of mesopores. The optical micrographs of these two particle samples (Figure 4) showed that both beads were opaque, indicating the presence of pores in their structures. The SEM images of these two copolymers (Figure 4) also indicated that Sty/VBC/DVB (4) had larger pores than Sty/VBC/DVB (3), confirming the data on pore diameter distribution of these two particles (Figure 5).

The Hildebrand solubility parameter, the square of the cohesive energy density, can be considered an indirect measurement of inter and intramolecular interactions between solvent and polymer molecules. The ratio between Hildebrand solubility parameters of the solvents (δs) and polymers (δp) can be used to predict whether a determined solvent is a solvating or non-solvating solvent of a determined polymer[29,40]. Several studies have indicated that the porosity characteristics of these copolymers is closely related to the thermodynamic relationship between the solubility parameters of solvents employed as porogenic agents and the polymeric chains formed during the polymerization[41-48]. In general, toluene ((δs 8.9 cal cm^{-3})$^{1/2}$) and heptane ((δs 7.4 (cal cm^{-3})$^{1/2}$) are classified as a solvating and non-solvating solvents of crosslinked polystyrene ((δs 8.5-9.3 cal cm^{-3})$^{1/2}$) respectively[40]. When diluent mixtures are employed as porogenic agents, the solubility parameter of the mixture (δmix) can be calculated as the average of the parameters of the pure diluents[43].

Influence of Textural Properties of Divinylbenzene Copolymers on the Immobilization of Lipase B from
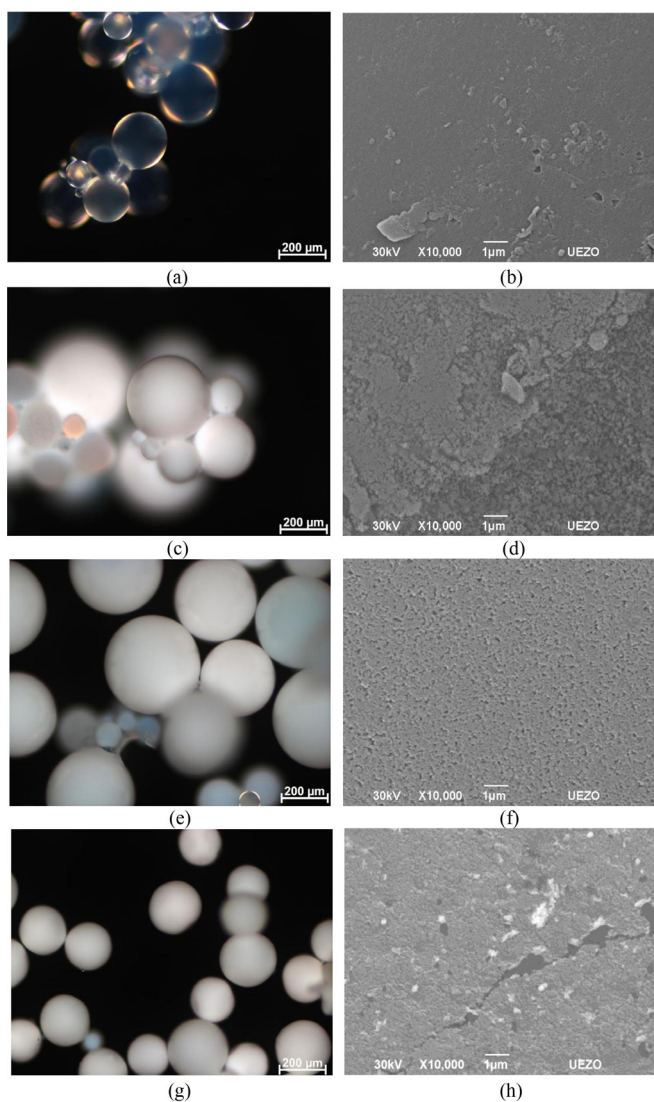*Candida antarctica*

7

Figure 4. Figure 3. Optical (OM) and scanning electron (SEM) microscopies of the copolymers Sty/DVB (1) OM: (a), SEM: (b); Sty/DVB (2) OM: (c), SEM: (d); Sty/VBC/DVB (3) OM: (e), SEM: (f) and Sty/VBC/DVB (4) OM: (g), SEM: (h).

When the polymerization of Sty/DVB or Sty/VBC/DVB was conducted in the presence of a mixture containing a higher proportion of solvating solvent (toluene), probably the phase separation process occurred after the gel point, via υ-induced syneresis, which normally leads to the formation of polymers with high specific surface areas and small pore diameters. On the other hand, when these polymerization reactions were conducted in the presence of a mixture containing a higher proportion of a non-solvating solvent (n-heptane), the phase separation process occurred before the gel point, via χ-induced syneresis, leading to the generation of polymer structures with high pore diameters associated with low specific surface areas[33,34].

It is also important to consider the agglomeration process of primary precipitated particles during the formation of polymer beads through aqueous suspension polymerization. First, it must be emphasized that crosslinked nuclei (10^2 Å in diameter) are generated continuously during polymerization.

The empty spaces between these precipitated nuclei are micropores (< 20 Å). Subsequently, the reaction between vinyl groups present on the surfaces of these nuclei results in agglomeration of the primary precipitated particles, generating microspheres (10^3 Å in diameter) that agglomerate, generating the larger domains (2,500-10,000 Å) of the final beads. The high content of n-heptane in the porogenic mixture (a non-solvating solvent) contributes to the formation of larger clusters of these primary precipitated nuclei and microspheres, generating particles with larger pore diameters[34].

Analysis of published specific surface areas, pore volumes, and average pore diameters of Sty/DVB copolymer microparticles indicates that increasing the relative amount of non-solvating solvent (heptane) in the diluent mixture can cause two important consequences:

(i) increase of average pore diameter with simultaneous increase of pore volume and surface area[45-49] in the
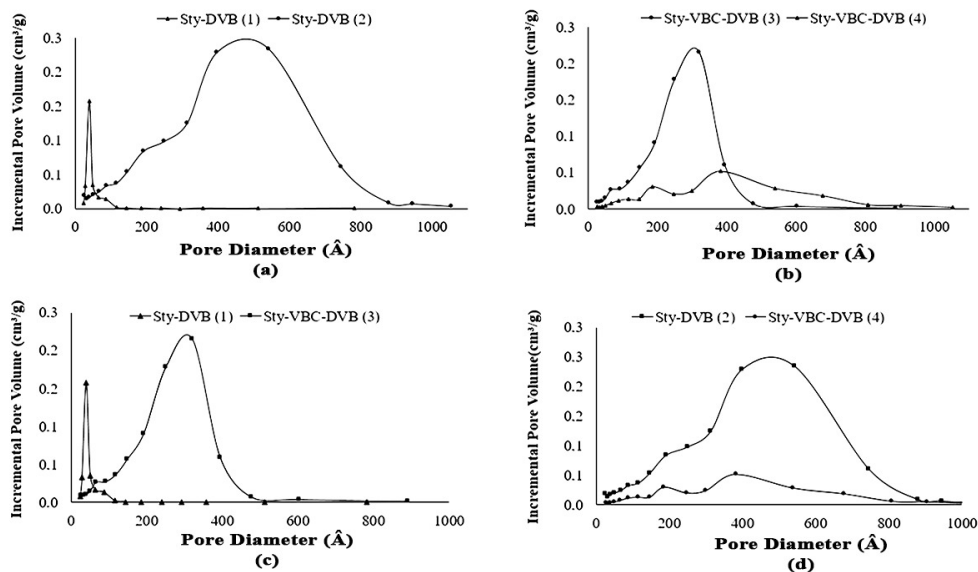
Figure 5. Pore size distributions of the supports: (a) Sty/DVB (1) x Sty/DVB (2); (b) Sty/VBC/DVB (3) x Sty/VBC/DVB (4); (c) Sty/DVB (1) x Sty/VBC/DVB (3); (d) Sty/DVB (2) x Sty/VBC/DVB (4).

presence of low DVB proportion in the monomeric mixture; or (ii) increase of average pore diameter with a decrease of pore volume and surface area in the presence of high DVB proportion in the monomeric mixture[47,48]. Therefore, the increase of the non-solvating solvent content can cause the formation of larger pore diameters, due to the higher average distances between the clusters of primary nuclei and microspheres. Below a determined limit, the increase of the average pore diameters is accompanied by an increase of the number of pores; above this limit, the increase of pore diameter can lead to a reduction of the pore volume as a consequence of the formation of larger clusters of primary nuclei and microspheres[34].

Comparison of data on specific surface area and pore volume of copolymers Sty/DVB (1) and Sty/VBC/DVB (3), prepared by using a mixture 80/20 v/v of toluene and n-heptane as diluent and 0.18 mol of DVB on monomeric composition (Table 2), indicated that the addition of 20% VBC in the monomeric mixture (substituting part of the volume of Sty), was associated with a significant reduction of the surface area and pore volume of the particles. The same observation applied when comparing the copolymers Sty/DVB (2) and Sty/VBC/DVB (4), prepared by using a mixture 20/80 v/v of toluene and n-heptane as diluent. Data on Hildebrand solubility parameters of VBC monomer are not available. However, we suppose that the presence of polar bond C-Cl in the VBC molecule can induce opposite charges of Sty, DVB and solvent molecules. The molecular interactions are weak, but in this case these interactions likely were sufficient to cause variations in the phase separation mechanism. Probably due to the presence of dipole-induced interactions between the molecules, the phase separation process occurred before the gel point, via χ-induced syneresis, resulting in a

reduction of the surface area accompanied by an increase in pore diameter of the particles.

Pore size distribution curves of the copolymers Sty/DVB (1) and Sty/VBC/DVB (3) (prepared by using as diluent a mixture with a higher proportion of toluene) shifted to higher diameters when VBC was added to the monomeric mixture, substituting part of the Sty monomer (Figure 5). However, this was not clearly observed by comparing the curves of the pore size distribution for Sty/DVB (2) and Sty/VBC/DVB (4) particles, prepared by employing a mixture containing a higher proportion of n-heptane as porogenic agent. We assume that since this type of mixture contributes to the preparation of particles with higher diameters, the effect of the presence of VBC on the pore diameters of the particles is not easily discerned.

The effect of VBC on the textural properties of Sty-DVB copolymers has been studied in the literature.

3.2. Effects of support morphology on the immobilization parameters of CALB

A consensus exits that the morphological characteristics and composition of polymeric supports can affect the catalytic properties of the derived biocatalysts, including stability, activity, selectivity and specificity[22,24,49,50]. Nevertheless, few studies have reported the relationship between the textural properties of the supports and the performance of biocatalysts prepared with lipases[4,22-26].

The immobilization kinetics of CALB on the analyzed supports was followed by evaluating the hydrolytic activity of the supernatant during the immobilization process, as shown in Figure 6. After a short period of contact between the Sty/DVB particles and the enzyme solution (0.5 h), immobilization yields (IY) of 84.6% and 98.7% were achieved, as shown in Figure 6. However, for the Sty/VBC/DVB particles, lower immobilization efficiencies were obtained, corresponding to
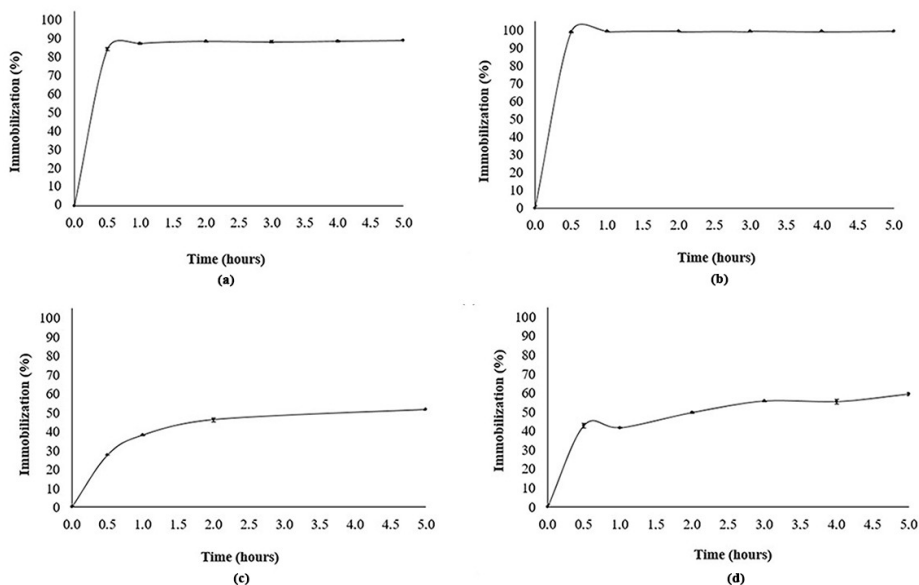
Influence of Textural Properties of Divinylbenzene Copolymers on the Immobilization of Lipase B from *Candida antarctica*

9

Figure 6. Kinetics of enzyme immobilization on the analyzed copolymer particles: (a) Sty/DVB (1) and (b) Sty/DVB (2); (c) Sty/VBC/DVB (3) and (d) Sty/VBC/DVB (4).

IY values of 50 to 60%, after longer contact times with the enzyme solution, as also shown in Figure 6. The biocatalysts prepared with Sty/DVB particles also resulted in higher recovered activities (Ra) and hydrolytic activities than the biocatalysts prepared with Sty/VBC/DVB particles, as shown in Table 3.

Sty/VBC/DVB copolymers are less hydrophobic than Sty/DVB copolymers, due to the presence of the monomer VBC, which is more polar than styrene and divinylbenzene monomers[51]. It is generally accepted that hydrophobic supports favor the open conformation of lipases, causing greater exposure of the active sites of the enzyme and increasing the activity of the heterogeneous biocatalysts produced[9].

Hydrophobic adsorption is normally based on interactions between the hydrophobic surface of the support and hydrophobic regions of the enzyme (concentrated around the active site and on the amphipathic face)[52]. However, some studies have reported the existence of ambiguous correlation between the degree of hydrophobicity of the supports and the final activity of the produced biocatalysts. For instance, Cipolatti et al.[31] reported that core-shell PMMA/PMMA particles generated biocatalysts with higher immobilization yields, recovered activities, and hydrolytic and esterification activities than biocatalysts produced with more hydrophobic monomers, such as PMMA-*co*-DVB/ PMMA-*co*-DVB and PS-*co*-DVB/PS-*co*-DVB. These results were explained considering that the presence of more hydrophilic monomers favored the diffusion of substrates and products through this matrix, resulting in higher enzymatic activities. Pinto et al.[22,23] reported two different behaviors, depending on the morphological characteristics of the supports: (i) for non-porous particles, they observed the absence of correlation between the degree of hydrophobicity and the biocatalyst activity; and (ii) for porous particles,

they observed higher correlation between the degree of hydrophobicity and the biocatalyst activity. The authors also observed that the performance of the biocatalysts could be closely related to the nonlinear synergetic interaction term between the degree of hydrophobicity and porosity of the particles. The increase of hydrophobicity contributed to the increase of the biocatalytic activity. However, as shown by Pinto et al.[23], highly hydrophobic surfaces increased the mass transfer limitations for the diffusion of substrates and products, causing a decrease of biocatalyst activities.

The Sty/DVB particles (2), with a higher specific surface area and pore diameter, and containing broader pore distributions (Figure 5a), provided higher IY values than the Sty/DVB particles (1). Sty/VBC/DVB particles (4), containing larger pores (Figure 5b), but lower specific surface area and porosity, provided higher IY values than the Sty/DVB particle (1). This result indicates that IY values tend to increase with the pore diameters, which can be more influential for IY values than the specific surface area of these particles. This result can be explained by the fact that larger pore diameters favor the access of the enzyme solution into the internal porous structure of the supporting particles.

Table 3 shows, however, that this behavior was not uniform, since the amount of enzyme added at the beginning of the immobilization procedure can also affect the final IY values. Pinto et al.[22], for instance, showed that supports prepared with the same comonomer composition, such as PS/P(S-*co*-DVB), and PS/PS core/shell particles, but with different specific surface areas and pore diameters, provided similar IY values. Besides this, Pinto et al.[24] reported that supports with high IY values (99.2%) and produced with polystyrene presented high surface areas (27.3 m^2 g^{-1}), although other supports with much smaller surface areas (2.9 - 13.1 m^2 g^{-1}) and pore volumes (0.03 - 0.09 cm^3 g^{-1})

Table 3. Specific surface areas (S), pore volumes (Vp) and average pore diameters(D) of copolymers and respective immobilization yields (IY), recovered activities (Ra) and hydrolytic activities (HA) of immobilized biocatalysts.

Supports	S [$m^2 g^{-1}$]	Vp [$cm^3 g^{-1}$]	D [Å]	YI [%]	Ra [%]	HA [$U g_{bio}^{-1}$]	Reference
Sty/DVB (1)	285	0.27	41.4	89.5	5.4	8.7 ± 1.2	
Sty/DVB (2)	319.2	1.06	186.8	99.2	14.3	25.6 ± 0.3	This work
Sty/VBC/DVB (3)	193.2	0.74	162.5	52.5	8.0	7.5 ± 0.6	
Sty/VBC/DVB (4)	48.9	0.24	179.6	59.3	3.4	3.6 ± 1.2	
(P(S-co-DVB) nanoparticles	113	0.28	128	74.5	1.5	4,6	
Sty/DVB (P(S-co-DVB)/ P(S-co-DVB))	43.4	0.23	212.9	97.8	2.3	9.3	5
Sty/DVB (Polystyrene 1)	27.3	0.20	287.6	99.2	1.8	2.3	
Sty/DVB (Polystyrene 3)	7.8	0.06	300.9	98.4	3.6	4.2	
Sty/DVB (Polystyrene 8)	2.9	0.03	400.8	94.2	2.4	1.9	
Sty/DVB (Polystyrene 9)	6.5	0.05	341.4	93.2	1.5	1.1	30
Sty/DVB (Polystyrene 11)	11.2	0.08	299.7	97.4	1.2	1.0	
Sty/DVB (Polystyrene 14)	13.1	0.09	263.7	90.9	2.2	1.6	
Sty/DVB (PS/P(S-co-DVB))	18.3	0.112	217.8	80	nd	2.5	
Sty/DVB (PS/PS)	1.6	0.013	357.5	82	nd	3.2	28
Sty/DVB (PS/PS)	7.9	Nd	218.8	52	nd	9	
Sty/DVB (PS-co-DVB/ PS-co-DVB)	19.4	Nd	152.5	61	nd	21	31
Sty/DVB (PS-co-DVB/ PS-co-DVB)	48.2	0.29	253.1	31.4	47.2	18.25	36
Accurel MP 1000	39.0	Nd	230.0	100	5.1	2.4	
PS/PMMA 2	8.7	Nd	272.3	100	11.1	4.6	
PS/PMMA 4	3.4	Nd	354.0	22.6	34.3	2.4	31
PS/PS-co-PC	6.2	Nd	251.2	100	14.5	6.8	
PMMA/PS 2	36.7	Nd	141.2	98.8	3.4	1.4	
PMMA/PS 4	0.2	Nd	195.0	100	5.8	2.4	

also provided biocatalysts with high IY values. The authors attributed this behavior to the unrestricted diffusion of the enzymes into the inner porous structure of the particles due to the small dimensions of the enzyme (30Å x 40Å x 50Å, molecular mass of about 33 KDa)[53,54] and the relatively high pore diameters of the mesoporous and macroporous polymer materials. Consequently, although it may be true that IY values can depend strongly on the morphological

Influence of Textural Properties of Divinylbenzene Copolymers on the Immobilization of Lipase B from
Candida antarctica

11

characteristics of the supports, the chemical characteristics of the material and the initial concentrations of enzymes in the immobilization solution can also have a significant influence on the final IY values.

Although high IY values were achieved with the Sty/DVB and Sty/VBC/DVB particles, the biocatalysts produced using these supports showed low recovered activities (Figure 7), confirming the results presented previously for other materials (Table 3). The lower retention of activity can be attributed to the lower availability of active sites. Another important factor that must be considered is the reduction of the molecular mobility or stiffening of the enzyme molecules in comparison with the native enzyme, which can explain the lower retention of activity[53]. The support characteristics and dimensions can lead to distortion of the immobilized enzyme molecules and consequently to inactivation of the active sites of the immobilized enzymes during the interaction with the hydrophobic surfaces, affecting the thermodynamic balance between lid and lid-holder enzyme conformations[23,55] and induced-dipole interactions of the lid with the hydrophobic surface of the polymer. Additionally, the possible formation of dimers between enzyme molecules can impair the activity of the immobilized enzymes[2,31,32].

The biocatalyst prepared with Sty/DVB particles (2), presenting higher pore diameters, pore volumes and specific surface areas provided higher recovered activity (Ra) and hydrolytic activity (HA) than the biocatalyst prepared with Sty/DVB particles (1). However, the biocatalyst prepared with Sty/VBC/DVB particles (3), presenting lower pore diameters but higher pore volumes and specific surface areas, generated biocatalysts with higher recovered activity (Ra) and hydrolytic activity (HA) than the biocatalyst produced with Sty/VBC/DVB particles (4). Therefore, for these supports, the surface area and pore volume exerted stronger influence on the hydrolytic activity and retained activity of the biocatalyst than the average pore diameter. Consequently, although the access of the enzyme molecules into the internal porous structure of the particles was controlled by the pore diameter, the access of reactants to enzymatic active sites arranged in a suitable conformation on the immobilized enzymes was controlled by the specific surface area and pore volume of the supports. As observed in the present work and reported in Table 3, supports presenting higher surface areas can provide biocatalysts with higher active enzymatic site contents that are more accessible to reactants.

The results reported in Table 3 show there is no consensus about the most influential morphological parameters of the supports (surface area, pore volume, and pore diameter) on the performance parameters Ra and HA. This is probably due to the complex network of reaction phenomena and the strong influence of small microenvironmental variations on the enzymatic activities. Cunha et al.[25] observed that biocatalysts prepared with core/shell P(S-co-DVB)/P(S-co-DVB) copolymer particles with high specific surface areas and small pore diameters had greater hydrolytic activities than biocatalysts prepared with supports with large surface areas and pore diameters, indicating that the surface area had a stronger influence on the hydrolytic activity of the biocatalyst than the pore diameter. Based on an empirical modeling approach, Pinto et al.[24] reported that the specific
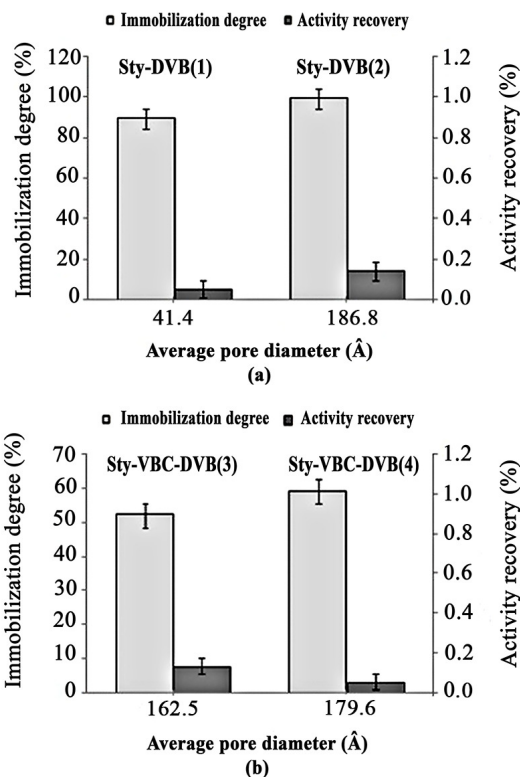

Figure 7. Immobilization yields (YI) and recovered activities (Ra) of the analyzed biocatalysts: (a) Sty/DVB biocatalysts and (b) Sty/VBC/DVB biocatalysts.

surface area exerted a stronger influence on the hydrolytic activity of biocatalysts than the pore diameter, which had a secondary effect on the analyzed biocatalyst activity. Li et al.[26] also reported that polystyrene beads with greater surface areas and smaller pore diameters provided biocatalysts with smaller activities than beads having smaller surface areas and larger pore diameters.

Based on these findings, it can be concluded that the distinct morphological features of the polymer support can exert significant and conflicting effects on the final biocatalyst performance, as discussed in the literature and presented in Table 3. For example, the surface area (which positively affects the activity of the immobilized enzymes) is normally expected to decrease with the increase of the average pore size (which positively affects the amounts of immobilized enzymes).

4. Conclusions

In the present work, spherical porous styrene/divinylbenzene (Sty/DVB) and styrene/vinylbenzyl chloride/divinylbenzene (Sty/VBC/DVB) particles with different textural characteristics were successfully prepared through aqueous suspension polymerization, employing mixtures of toluene (solvating solvent) and n-heptane (non-solvating solvent) as porogenic agents. In all cases, the obtained particles presented meso or macroporous characteristics. In the case of Sty/DVB

particles, the increase of the heptane content resulted in larger pore diameters, pore volumes, and specific surface areas. However, in the case of Sty/VBC/DVB particles, the increase of the heptane content caused the production of larger pore diameters and smaller specific pore volumes and surface areas.

Biocatalysts prepared with the Sty/DVB particles, more hydrophobic and with higher specific areas, presented greater immobilization yields (IY) than those prepared with Sty/VBC/DVB particles. Sty/DVB particles also yielded biocatalysts with higher recovered activities (Ra, 14.3%) and hydrolytic activities (HA, 25.6 U g_{bio}^{-1}) than biocatalysts prepared with the Sty/VBC/DVB particles. Although significantly higher IY values were achieved for all copolymers, the biocatalysts produced with these supports presented small Ra values, which can be due to the reduced molecular mobility, inappropriate geometrical orientation, and inactivation of active sites of the immobilized enzymes during the immobilization process. In particular, the increase of average pore diameter resulted in higher IY values (indicating the existence of geometrical constraints for immobilization of the enzymes), while Ra and HA values increased when the surface area and pore volume of the particles increased (indicating the importance of chemical interactions with the particle surfaces). Based on these findings, we can conclude that the distinct morphological features of the polymer support can exert significant and opposing effects on the final biocatalyst performance, since the specific surface area is normally expected to decrease with the increase of the average pore sizes.

5. Acknowledgements

6. References

1. Basso A, Serban S. Industrial applications of immobilized enzymes: a review. Mol. Catal. 2019;479:110607. http://dx.doi.org/10.1016/j.mcat.2019.110607.

2. Ferreira MM, Santiago FLB, Silva NAG, Luiz JHH, Fernandez-Lafuente R, Mendes AA, et al. Different strategies to immobilize lipase from *Geotrichum candidum*: kinetic and thermodynamic studies. Process Biochem. 2018;67:55-63. http://dx.doi.org/10.1016/j.procbio.2018.01.028.

3. Gao Z, Chu J, Jiang T, Xu T, Wu B, He B. Lipase immobilization on functionalized mesoporous TiO2: specific adsorption, hyperactivation and application in cinnamyl acetate synthesis. Process Biochem. 2018;64:152-9. http://dx.doi.org/10.1016/j.procbio.2017.09.011.

4. Pinto MCC, Castro NLS, Cipolatti EP, Fernandez-Lafuente R, Manoel EA, Freire DMG, et al. Effects of reaction operation policies on properties of core-shell polymer supports used for preparation of highly active biocatalysts. Macromol React Eng. 2018;13(1):1800055. http://dx.doi.org/10.1002/mren.201800055.

5. Kapoor M, Gupta MN. Lipase promiscuity and its biochemical applications. Process Biochem. 2012;47(4):555-69. http://dx.doi.org/10.1016/j.procbio.2012.01.011.

6. Xing X, Jia J-Q, Zhang J-F, Zhou Z-W, Li J, Wang N, et al. CALB immobilized onto magnetic nanoparticles for efficient kinetic resolution of racemic secondary alcohols: long-term stability and reusability. Molecules. 2019;24(3):490. http://dx.doi.org/10.3390/molecules24030490.

7. Wahab RA, Elias N, Abdullah F, Ghoshal SK. On the taught new tricks of enzymes immobilization: an all-inclusive overview. React Funct Polym. 2020;152:104613. http://dx.doi.org/10.1016/j.reactfunctpolym.2020.104613.

8. Cipolatti EP, Pinto MCC, Henriques RO, Pinto JCCS, Castro AM, Freire DMG, et al. Enzymes in green chemistry: the state of the art in chemical transformations. In: Singh RS, Singhania RR, Pandey A, Larroche C, editors. Advances in enzyme technology: biomass, biofuels, biochemicals. Amsterdam: Elsevier; 2019. Chapter 5. http://dx.doi.org/10.1016/B978-0-444-64114-4.00005-4.

9. Rodrigues RC, Virgen-Ortíz JJ, Santos JCS, Berenguer-Murcia A, Alcantara AR, Barbosa O, et al. Immobilization of lipases on hydrophobic supports: immobilization mechanism, advantages, problems, and solutions. Biotechnol Adv. 2019;37(5):746-70. http://dx.doi.org/10.1016/j.biotechadv.2019.04.003. PMid:30974154.

10. Maksin DD, Nastasović AB, Milutinović-Nikolić AD, Suručić LT, Sandić ZP, Hercigonja RV, et al. Equilibrium and kinetics study on hexavalent chromium adsorption onto diethylene triamine grafted glycidyl methacrylate based copolymers. J Hazard Mater. 2012;209-210:99-110. http://dx.doi.org/10.1016/j.jhazmat.2011.12.079.

11. Silva MVC, Aguiar LG, Castro HF, Freitas L. Optimization of the parameters that affect the synthesis of magnetic copolymer styrene-divinilbenzene to be used as efficient matrix for immobilizing lipases. World J Microbiol Biotechnol. 2018;34(11):169. http://dx.doi.org/10.1007/s11274-018-2553-1.

12. Bento HBS, Castro HF, Oliveira PC, Freitas LJ. Magnetized poly(STY-co-DVB) as a matrix for immobilizing microbial lipase to be used in biotransformation. Magn. Magn. Mater. 2017;426:95-101. http://dx.doi.org/10.1016/j.jmmm.2016.11.061.

13. Li D, Wang W, Liu P, Xu L, Faiza M, Yang B, et al. Immobilization of *Candida antarctica* lipase B onto ECR1030 resin and its application in the synthesis of n-3 PUFA-rich triacylglycerols. Eur J Lipid Sci Technol. 2017;119(12):1700266. http://dx.doi.org/10.1002/ejlt.201700266.

14. Abreu L, Fernandez-Lafuente R, Rodrigues RC, Volpato G, Aybub MAZ. Efficient purification-immobilization of an organic solvent-tolerant lipase from Staphylococcus warneri EX17 on porous styrene-divinylbenzene beads. J Mol Catal, B Enzym. 2014;99:51-5. http://dx.doi.org/10.1016/j.molcatb.2013.10.018.

15. Mihailovic M, Stojanovic M, Banjanac K, Carevic M, Prlainovic N, Milosavic N, et al. Immobilization of lipase on epoxy-activated Purolite® A109 and its post-immobilization stabilization. Process Biochem. 2014;49(4):637-46. http://dx.doi.org/10.1016/j.procbio.2014.01.013.

16. Martins AB, Friedrich JLR, Cavalheiro JC, Garcia-Galan C, Barbosa O, Ayub MAS, et al. Improved production of butyl butyrate with lipase from Thermomyces lanuginosus immobilized on styrene–divinylbenzene beads. Bioresour Technol. 2013;134:417-22. http://dx.doi.org/10.1016/j.biortech.2013.02.052.

17. Poppe JK, Garcia-Galan C, Matte CR, Fernandez-Lafuente R, Rodrigues RC, Ayub MAZ. Optimization of synthesis of fatty acid methyl esters catalyzed by lipase B from *Candida antarctica* immobilized on hydrophobic supports. J Mol Catal, B Enzym. 2013;94:51-6. http://dx.doi.org/10.1016/j.molcatb.2013.05.010.

18. Liu T, Liu Y, Wang X, Li Q, Wang J, Yan Y. Improving catalytic performance of *Burkholderia cepacia* lipase immobilized on macroporous resin NKA. J Mol Catal, B Enzym. 2011;71(1-2):45-50. http://dx.doi.org/10.1016/j.molcatb.2011.03.007.

19. Yücel Y, Demir C, Dizge N, Keskinler B. Lipase immobilization and production of fatty acid methyl esters from canola oil using immobilized lipase. Biomass Bioenergy. 2011;35(4):1496-501. http://dx.doi.org/10.1016/j.biombioe.2010.12.018.

Influence of Textural Properties of Divinylbenzene Copolymers on the Immobilization of Lipase B from *Candida antarctica*

13

20. Aybastier Ö, Demir C. Optimization of immobilization conditions of Thermomyces lanuginosus lipase on styrene–divinylbenzene copolymer using response surface methodology. J Mol Catal, B Enzym. 2010;63(3-4):170-8. http://dx.doi.org/10.1016/j.molcatb.2010.01.013.

21. Illanes A. Enzyme biocatalysis: principles and applications. Valparaíso: Springer. 2008. http://dx.doi.org/10.1007/978-1-4020-8361-7.

22. Pinto MCC, Everton SS, Cirilo LCM, Cipolatti EP, Manoel EA, Pinto JC, et al. Effect of hydrophobicity degree of polymer particles on lipase immobilization and on biocatalyst performance. Biocatal Biotransform. 2020;38:304-14. http://dx.doi.org/10.1080/10242422.2020.1739026.

23. Pinto MCC, Cipolatti EP, Manoel EA, Freire DMG, Becer ÇR, Pinto JC. Production of new functionalized polymer nanoparticles and use for manufacture of novel nanobiocatalysts. Macromol Mater Eng. 2020;305(6):e2000065. http://dx.doi.org/10.1002/mame.202000065.

24. Pinto MCC, Freire DMG, Pinto JC. Influence of the morphology of core-shell supports on the Immobilization of lipase B from *Candida antarctica*. Molecules. 2014;19(8):12509-30. http://dx.doi.org/10.3390/molecules190812509.

25. Cunha AG, Besteti MD, Manoel EA, Silva AAT, Almeida RV, Simas ABC, et al. Preparation of core-shell polymer supports to immobilize lipase B from *Candida antarctica*: effect of the support nature on catalytic properties. J Mol Catal, B Enzym. 2014;100:59-67. http://dx.doi.org/10.1016/j.molcatb.2013.11.020.

26. Li Y, Gao F, Wei W, Qu J-B, Ma GH, Zhou WQ. Pore size of macroporous polystyrene microspheres affects lipase immobilization. J Mol Catal, B Enzym. 2010;66(1-2):182-9. http://dx.doi.org/10.1016/j.molcatb.2010.05.007.

27. Torquato ECC, Brito APN, Trovão RS, Oliveira MA, Smith NS, Pinto MCC, et al. Synthesis of porous polymeric supports with PolyHIPE structures based on styrene-divinylbenzene copolymers. Macromol Symp. 2020;394(1):2000109. http://dx.doi.org/10.1002/masy.202000109.

28. Teixeira VG, Coutinho FMB, Gomes AS. Principais métodos de caracterização da porosidade de resinas à base de divinilbenzeno. Quim Nova. 2001;24(6):808-18. http://dx.doi.org/10.1590/S0100-40422001000600019.

29. Costa LC, Monteiro RC, Castro HMA, Ribeiro TS, Oliveira MA, Torquato ECC, et al. Glycidyl methacrylate-ethylene glycol dimethacrylate copolymers with varied pore structures prepared with different reaction parameters. Mater Res. 2020;23(3):e20190550. http://dx.doi.org/10.1590/1980-5373-mr-2019-0550.

30. ASTM: American Society for Testing and Materials. Annual book of ASTM. Philadelphia: ASTM; 1975. Part. 35, ASTM D I895-69: apparent density, bulk factor and pourability of plastic materials.

31. Cipolatti EP, Pinto MCC, Robert JM, Silva TP, Beralto TC, Santos JGF, et al. Pilot-scale development of core–shell polymer supports for the immobilization of recombinant lipase B from *Candida antarctica* and their application in the production of ethyl esters from residual fatty acids. J Appl Polym Sci. 2018;135(40):46727. http://dx.doi.org/10.1002/app.46727.

32. Manoel EA, Robert JM, Pinto MCC, Machado ACO, Besteti MD, Coelho MAS, et al. Evaluation of the performance of differently immobilized recombinant lipase B from *Candida antarctica* preparations for the synthesis of pharmacological derivatives in organic media. RSC Adv. 2016;6(5):4043-52. http://dx.doi.org/10.1039/C5RA22508F.

33. Gokmen MT, Du Prez FE. Porous polymer particles- A comprehensive guide to synthesis, characterization, functionalization and applications. Prog Polym Sci. 2012;37(3):365-405. http://dx.doi.org/10.1016/j.progpolymsci.2011.07.006.

34. Okay O. Macroporous copolymer networks. Prog Polym Sci. 2000;25(6):711-79. http://dx.doi.org/10.1016/S0079-6700(00)00015-0.

35. Sing KSW, Everett DH, Haul RAW, Moscou L, Pierotti RA, Rouquerol J, et al. Reporting physisorption data for Gas/Solid systems with special reference to the determination of surface area and porosity. (Recommendations 1984). Pure Appl Chem. 1985;1985(57):603-19. http://dx.doi.org/10.1351/pac198557040603.

36. Thielemann JP, Girgsdies F, Schlögl R, Hess C. Pore structure and surface area of silica SBA-15: influence of washing and scale-up. Beilstein J Nanotechnol. 2011;2:110-8. http://dx.doi.org/10.3762/bjnano.2.13.

37. Thommes M, Kaneko K, Neimark AV, Olivier AV, Rodriguez-Reinoso F, Rouquerol J, et al. Physisorption of gases, with special reference to the evaluation of surface area and pore size distribution (IUPAC Technical Report). Pure Appl Chem. 2015;87(9-10):1051-69. http://dx.doi.org/10.1515/pac-2014-1117.

38. Zhang Y, Shao D, Yan J, Jia X, Li Y, Yu P, et al. The pore size distribution and its relationship with shale gas capacity in organic-rich mudstone of Wufeng-Longmaxi Formations, Sichuan Basin, China. Nat. Gas. Geosci. 2016;1(3):213-20. http://dx.doi.org/10.1016/j.jnggs.2016.08.002.

39. Zheng Y, Wang Q, Yang C, Qiu T. Experimental study on mass transport mechanism in poly (styrene-co-divinylbenzene) microspheres with hierarchical pore structure. Chem Eng Process. 2019;139:183-92. http://dx.doi.org/10.1016/j.cep.2019.03.016.

40. Grulke EA. Solubility parameter values. In: Brandrup J, Immergut EH, Grulke EA, editors. The Wiley database of polymer properties. Lexington: John Wiley & Sons; 1999. Vol. 7. http://dx.doi.org/10.1002/0471532053.bra062.

41. Costa LC, Gomes AS, Coutinho FMB, Teixeira VG. Chelating resins for mercury extraction based on grafting of polyacrylamide chains onto styrene-divinylbenzene copolymers by gamma irradiation. React Funct Polym. 2010;70(10):738-46. http://dx.doi.org/10.1016/j.reactfunctpolym.2010.07.003.

42. Coutinho FMB, Souza RR, Gomes AS. Synthesis, characterization and evaluation of sulfonic resins as catalysts. Eur Polym J. 2004;40(7):1525-32. http://dx.doi.org/10.1016/j.eurpolymj.2004.02.003.

43. Coutinho FMB, Luz La Torre M, Rabelo D. Cosolvency effect on the porous structure formation of styrene divinylbenzene copolymers. Eur Polym J. 1998;34(5-6):805-8. http://dx.doi.org/10.1016/S0014-3057(97)00195-X.

44. Kangwansupamonkon W, Damronglerd S, Kiatkamjornwong S. Effects of the crosslinking agent and diluents on bead properties of styrene-divinylbenzene copolymers. J Appl Polym Sci. 2002;85(3):654-9. http://dx.doi.org/10.1002/app.10620.

45. Coutinho FMB, Rezende SM. Catalisadores sulfônicos imobilizados em polímeros: síntese, caracterização e avaliação. Polímeros. 2001;11(4):222-33. http://dx.doi.org/10.1590/S0104-14282001000400012.

46. Neves MAFS, Dias ML, Coutinho FMB. Copolímeros de estireno-divinilbenzeno para aplicação em cromatografia de exclusão por tamanho. Polímeros. 1997;7(3):71-7. http://dx.doi.org/10.1590/S0104-14281997000300011.

47. Coutinho FMB, Cunha L, Gomes AS. Suportes poliméricos para catalisadores sulfônicos: síntese e caracterização. Polímeros. 2004;14(1):31-7. http://dx.doi.org/10.1590/S0104-14282004000100011.

48. Santa Maria LC, Aguiar MRMP, Guimarães PIC, Amorim MCV, Costa MAS, Almeida RSM, et al. Synthesis of crosslinked resin based on methacrylamide, styrene and divinylbenzene obtained from polymerization in aqueous suspension. Eur Polym J. 2003;39(2):291-6. http://dx.doi.org/10.1016/S0014-3057(02)00196-9.

49. Graebin NG, Martins AB, Lorenzoni ASG, Garcia-Galan R, Fernandez-Lafuente R, Ayub MAS, et al. Immobilization of lipase B from *Candida antarctica* on porous styrene–divinylbenzene beads improves butyl acetate synthesis. Biotechnol Prog. 2012;28(2):406-12. http://dx.doi.org/10.1002/btpr.1508.

50. Fernandez-Lorente G, Cabrera Z, Godoy C, Fernandez-Lafuente R, Palomo JM, Guisan JM. Interfacially activated lipases against hydrophobic supports: effect of the support nature on the biocatalytic properties. Process Biochem. 2008;43(10):1061-7. http://dx.doi.org/10.1016/j.procbio.2008.05.009.

51. Liu Q, Xia B, Huang J, Liao B, Liu H, Ou B, et al. Hypercrosslinked polystyrene microspheres with ultrahigh surface area and their application in gas storage. Mater Chem Phys. 2017;199:616-22. http://dx.doi.org/10.1016/j.matchemphys.2017.07.032.

52. Cao L. Carrier-bound immobilized enzymes: principles, application and design. Weinheim: Wiley-VCH; 2005. http://dx.doi.org/10.1002/3527607668.

53. Strzelczyk P, Bujacz GD, Kiełbasiński P, Błaszczyk J. Crystal and molecular structure of hexagonal form of lipase B from *Candida antarctica*. Acta Biochim Pol. 2016;63(1):103-9. http://dx.doi.org/10.18388/abp.2015_1065.

54. Uppenberg J, Hansen MT, Patkar S, Jones TA. The sequence, crystal structure determination and refinement of two crystal forms of lipase B from Candida antarctica. Structure. 1994;2(4):293-308. http://dx.doi.org/10.1016/S0969-2126(00)00031-9.

55. Luan B, Zhou R. Novel self-activation mechanism of *Candida antarctica* lipase B. Phys Chem Chem Phys. 2017;19(24):15709-14. http://dx.doi.org/10.1039/C7CP02198D.